

# Microwave dielectric properties of doped $\text{Ba}_{6-x}(\text{Sm}_{1-y}, \text{Nd}_y)_{8+2x/3}\text{Ti}_{18}\text{O}_{54}$ oxides

P. LAFFEZ\*, G. DESGARDIN, B. RAVEAU

Laboratoire de Cristallographie et Sciences des Matériaux, Institut des Sciences de la Matière et du Rayonnement-ISMRA, Boulevard du Maréchal Juin, 14050 Caen Cedex, France

Dielectric ceramic compositions for microwave applications belonging to the  $(\text{BaO})-(\text{Nd}_2\text{O}_3)-(\text{Sm}_2\text{O}_3)-(\text{TiO}_2)$  phase diagram were studied. Two compositions were selected for study, the doping effect of  $\text{MnO}_2$ ,  $\text{WO}_3$ ,  $\text{CaO}$  on dilatometry, microstructure and microwave properties. The effect of the nature and the amount of dopants on microstructure and microwave properties were clearly demonstrated. The effect of the addition of 1 or 2 wt%  $\text{WO}_3$ ,  $\text{MnO}_2$  and  $\text{CaO}$  to  $\text{Ba}_4(\text{Sm}_{0.6}, \text{Nd}_{0.4})_{9.33}\text{Ti}_{18}\text{O}_{54}$  and  $\text{Ba}_{3.75}(\text{Sm}_{0.5}, \text{Nd}_{0.5})_{9.5}\text{Ti}_{18}\text{O}_{54}$  was studied. It was found that these two compositions lead to dense ceramics exhibiting excellent microwave properties, for instance  $\epsilon = 74\text{--}81$ ,  $Q \times f$  up to 9000 GHz at 3 GHz and  $\tau_f$  around  $+9$  p.p.m.  $^\circ\text{C}^{-1}$ .

## 1. Introduction

Ceramics in  $\text{BaO}-\text{Nd}_2\text{O}_3-\text{TiO}_2$  and  $\text{BaO}-\text{Sm}_2\text{O}_3-\text{TiO}_2$  systems are well known as quite useful dielectric materials for applications at microwave frequencies. The properties and crystal chemistry in the system  $\text{BaO}-\text{Nd}_2\text{O}_3-\text{TiO}_2$ , especially in  $\text{TiO}_2$ -rich portions were studied in detail by Kolar [1, 2] while the  $\text{BaO}-\text{Sm}_2\text{O}_3-\text{TiO}_2$  system was explored by Kawashima [3] and Nishigaki *et al.* [4]. In a previous work [5] we reported the difficulty in controlling the temperature stability of the resonant frequency in the  $\text{BaO}-\text{Sm}_2\text{O}_3-\text{TiO}_2$  system, mainly due to the presence of secondary phases in ceramics with zero temperature coefficient of the resonant frequency,  $\tau_f$ , while pure matrix ceramics lead to negative  $\tau_f$ . In another paper [6] we pointed out the possibility of reaching nearly zero  $\tau_f$  by partial substitutions of samarium by neodymium compositions belonging to the theoretical bronzoïd line  $\text{Ba}_{6-x}\text{Ln}_{8+2x/3}\text{Ti}_{18}\text{O}_{54}$ .

The purpose of this study was to investigate the microstructure and dielectric properties at microwave frequencies for two ceramics having the composition  $\text{Ba}_{6-x}(\text{Sm}_{1-y}, \text{Nd}_y)_{8+2x/3}\text{Ti}_{18}\text{O}_{54}$  ( $x = 2$ ,  $y = 0.4$  and  $x = 2.25$ ,  $y = 0.5$ ) doped with different amounts of  $\text{WO}_3$ ,  $\text{MnO}_2$  and  $\text{CaO}$ . The aim was to reduce slightly the positive coefficient of the resonant frequency as close as possible to zero, while trying to increase the dielectric constant and decrease the dielectric losses. We chose the nature of the dopant by reference to different papers. Nishigaki *et al.* [7], reported that a small amount of  $\text{WO}_3$  added to  $\text{BaTi}_4\text{O}_9$  or  $\text{Ba}_2\text{Ti}_9\text{O}_{20}$  ceramics increased  $Q$  and decreased  $\tau_f$ . This improvement of the dielectric properties was attributed to the appearance of the  $\text{BaWO}_4$  phase for

which  $\tau_f$  is about  $-33$  p.p.m.  $^\circ\text{C}^{-1}$ . In our case, the bronzoïd type structure exhibits a tunnel structure related to the tetragonal tungsten bronze  $\text{A}_x\text{WO}_3$ . This suggests that doping with  $\text{WO}_3$  could “extract”  $\text{Ba}^{2+}$  cations and form  $\text{BaWO}_4$ . If that took place, the bronzoïd structure should release samarium, neodymium and titanium which could form  $(\text{Sm}, \text{Nd})\text{Ti}_2\text{O}_7$  which have negative  $\tau_f$  values too ( $\tau_f \approx -120$  p.p.m.  $^\circ\text{C}^{-1}$ , after Wakino *et al.* [8]).  $\text{MnO}_2$  dopant was found to lead to a large decrease of the temperature coefficient in  $\text{BaO}-\text{Nd}_2\text{O}_3-5\text{TiO}_2$  ceramics [9], while  $\epsilon$  increases, and  $Q$  decreases. The corresponding samples contained several unidentified phases. In  $\text{BaTi}_4\text{O}_9$ , an increase of the quality factor,  $Q$ , was noted by Mhaisalkar *et al.* [10] for the same dopant. This increase is attributed to the possible formation of a liquid phase during sintering which can improve the densification. Finally, an improvement in  $Q$  was also noted when doping  $\text{BaTi}_4\text{O}_9$  with  $\text{CaO}$  [10].

Our study concerns the addition of 1 and 2 wt%  $\text{WO}_3$ ,  $\text{MnO}_2$  and  $\text{CaO}$  to  $\text{Ba}_4(\text{Sm}_{0.6}, \text{Nd}_{0.4})_{9.33}\text{Ti}_{18}\text{O}_{54}$  and  $\text{Ba}_{3.75}(\text{Sm}_{0.5}, \text{Nd}_{0.5})_{9.5}\text{Ti}_{18}\text{O}_{54}$ .

## 2. Experimental procedure

### 2.1. Sample preparation

The appropriate amounts of  $\text{BaCO}_3$ ,  $\text{Sm}_2\text{O}_3$ ,  $\text{Nd}_2\text{O}_3$  and  $\text{TiO}_2$  were intimately mixed by attrition milling, and then calcined at  $950^\circ\text{C}$  in alumina boats. This calcination temperature leads to some intermediate phases, previously described [5, 6] ( $\text{BaTi}_4\text{O}_9$ ,  $\text{Sm}_2\text{Ti}_2\text{O}_7$ ,  $\text{Nd}_2\text{Ti}_2\text{O}_7$ , etc.). Those phases, when sintered, will be transformed to the final bronzoïd

\* Present address: Superconductivity Research Laboratory, International Superconductivity Technology Center, Shinonome 1-10-1, Koto-Ku, Tokyo 135, Japan.

ture. Furthermore, this process is said to eliminate, partially, anisotropy problems due to a uniaxially pressed sample [11]. The calcination is followed by a second attrition milling process in order to reach a homogeneous granulometric distribution close to 1  $\mu\text{m}$ . During this second attrition milling, the correct amount of dopant is added to the calcined powder. The powders mixed with an organic binder (PVA 5%) are pressed into the form of cylinders, at  $1\text{T cm}^{-2}$  and finally sintered at high temperature in an oxygen flow in a tubular furnace at a heating rate of  $200\text{ }^\circ\text{C h}^{-1}$ .

## 2.2. Characterization

The calcined powders and the sintered samples were characterized by X-ray diffraction (XRD) using a Guinier camera. Microstructure observations were carried out on polished samples by SEM, using a Jeol 840 microscope. For this purpose, a thermal treatment at  $1150\text{ }^\circ\text{C}$  for 5 min was performed to reveal the grain boundaries. The reactivity of the powders and the sintering phenomena were studied by dilatometry using a Adamec-Llomargy dilatometer (model DI 24). Microwave characteristics such as the dielectric constant,  $\epsilon$ , the product of quality factor and the resonant frequency,  $Q \times f$ , and the temperature coefficient of the resonant frequency,  $\tau_f$ , were determined at 3 GHz using the dielectric resonator method [12] at the Tekelec Microwave Company, France.

## 3. Results

### 3.1. $\text{Ba}_4(\text{Sm}_{0.6}\text{Nd}_{0.4})_{9.33}\text{Ti}_{18}\text{O}_{54}$ composition (labelled 1)

#### 3.1.1. Dilatometric study

Fig. 1 shows the evolution of the shrinkage in an

oxygen flow for a pellet corresponding to this composition, without dopant, calcined at  $950\text{ }^\circ\text{C}$ . The ordinary dilatation is not observed. Shrinkage starts at  $600\text{ }^\circ\text{C}$ , and continues until  $800\text{ }^\circ\text{C}$ . A bending of the curve is observed between  $1000$  and  $1150\text{ }^\circ\text{C}$ , corresponding to the formation of the bronzoïd  $\text{Ba}_{6-x}\text{Ln}_{8+2x/3}\text{Ti}_{18}\text{O}_{54}$ , as previously reported [5]. The shrinkage starts again at  $1150\text{ }^\circ\text{C}$ , and proceeds slowly until  $1200\text{ }^\circ\text{C}$  and then accelerates quickly after this temperature. During the plateau at  $1350\text{ }^\circ\text{C}$ , the shrinkage continues. No further evolution occurs during the cooling process.

*3.1.1.1.  $\text{WO}_3$  doped sample.* The dilatometric study of 2 wt % doped sample (Fig. 1) leads to a similar dilatometric curve compared to the undoped one, until  $600\text{ }^\circ\text{C}$ . The same onset of shrinkage as for the undoped sample is noted at that temperature, but it ceases at  $700\text{ }^\circ\text{C}$  instead of  $800\text{ }^\circ\text{C}$ . The shrinkage did not occur again until the formation of the bronzoïd at  $1000\text{ }^\circ\text{C}$ . Then, the shrinkage began  $50\text{ }^\circ\text{C}$  earlier and the densification rate was higher than for the undoped sample. A slight densification can be observed during the plateau at  $1400\text{ }^\circ\text{C}$ .

*3.1.1.2.  $\text{MnO}_2$  doped sample.* The dilatometric curve of the 2 wt % doped sample (Fig. 1) leads to a curve that exhibits almost no change until  $1080\text{ }^\circ\text{C}$ . At that temperature, the shrinkage began and accelerated very quickly between  $1100$  and  $1250\text{ }^\circ\text{C}$ . When the temperature reached  $1350\text{ }^\circ\text{C}$  the shrinkage was almost finished. According to Mhaisalkar *et al.* [10], it is possible that a liquid phase appears, improving

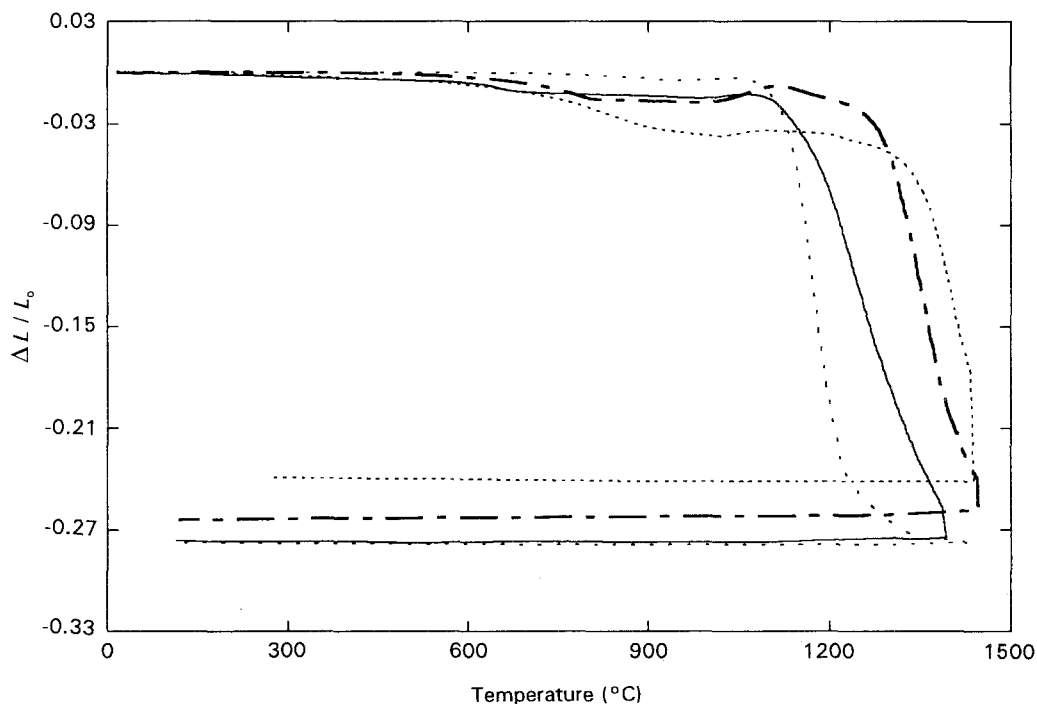


Figure 1 Shrinkage evolution of a pellet of composition  $\text{Ba}_4(\text{Sm}_{0.6}\text{Nd}_{0.4})_{9.33}\text{Ti}_{18}\text{O}_{54}$ : calcined at  $950\text{ }^\circ\text{C}$ , sintered in oxygen, with different dopants: (—) 2 wt %  $\text{WO}_3$ , (---) 2 wt %  $\text{MnO}_2$ , (···) 2 wt %  $\text{CaO}$ , (-·-·) no dopant.

the densification, but SEM observations did not reveal any evidence for the liquid-phase formation.

**3.1.1.3. CaO-doped sample.** The 2 wt % doped sample shows a dilatometric curve with the same characteristics as samples without dopant, but the signal is amplified and starts 50 °C. later. The sintering began after 1200 °C and started slowly. The shrinkage continues during the plateau. In that case it seems that doping with CaO causes the sintering, and a degradation of the microwave properties should be expected.

This dilatometric study led to the different samples being sintered with the following thermal cycles:

- (a) WO<sub>3</sub>-doped sample: sintered at 1450 °C for 2 h in oxygen;
- (b) MnO<sub>2</sub>-doped sample: sintered at 1350 °C for 2 h in oxygen;
- (c) CaO-doped sample: sintered at 1450 °C for 2 h in oxygen.

### 3.1.2. Influence of dopant on the microstructure

Fig. 2 shows the microstructure of ceramics sintered at various temperatures with an oxygen flow.

The undoped sample sintered at 1450 °C shows a pure matrix where secondary phases are not observed. The high sintering temperature leads to a good densification.

The two samples doped with two different amounts of WO<sub>3</sub> show the same microstructures as the undoped one.

Samples doped with 1 wt % MnO<sub>2</sub> show a pure ceramic. On the other hand, when the amount of MnO<sub>2</sub> increases (2 wt %), a secondary phase appears in the form of inclusions of a size centred around 1 µm. Because of this small size (1 µm), energy dispersive spectroscopic (EDS) analysis was not performed. A multitude of microcracks were visible for this sample at high magnification (see Fig. 2).

Finally, the CaO-doped sample leads to a pure matrix where a high porosity remains, according to the dilatometric study which showed the difficulty of sintering this kind of sample.

### 3.1.3. Microwave properties

Table I summarizes microwave characteristics of the different doped samples. The undoped one shows excellent dielectric properties,  $\epsilon = 77$ ,  $Q \times f = 9000$  GHz and  $\tau_f = +9$  p.p.m. °C<sup>-1</sup>.

**3.1.3.1. WO<sub>3</sub> effect.** The improved density of this sample in comparison with the undoped one, leads to a slightly higher dielectric constant. However, the quality factor decreases and the  $\tau_f$  increases. The phases BaWO<sub>4</sub> and (Sm, Nd)<sub>2</sub>Ti<sub>2</sub>O<sub>7</sub>, which were expected to lower the  $\tau_f$  to zero, did not appear.

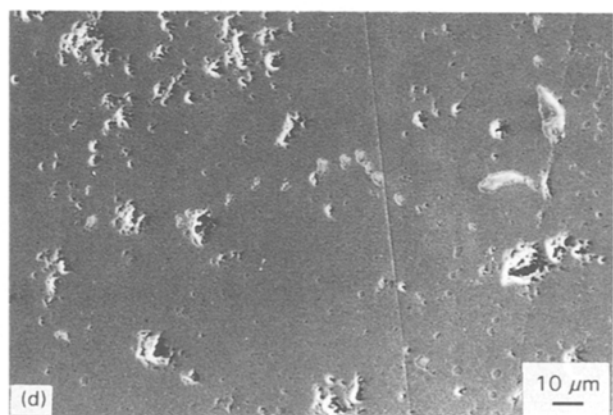
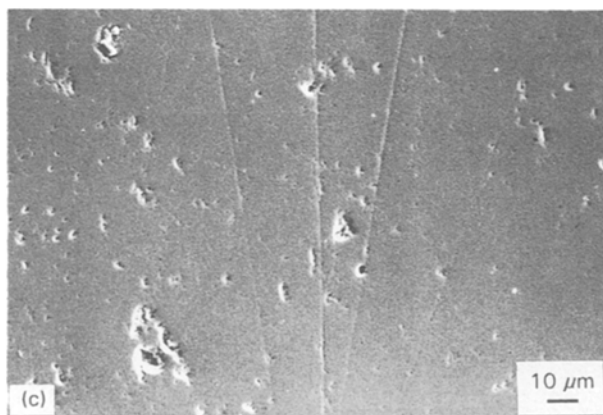
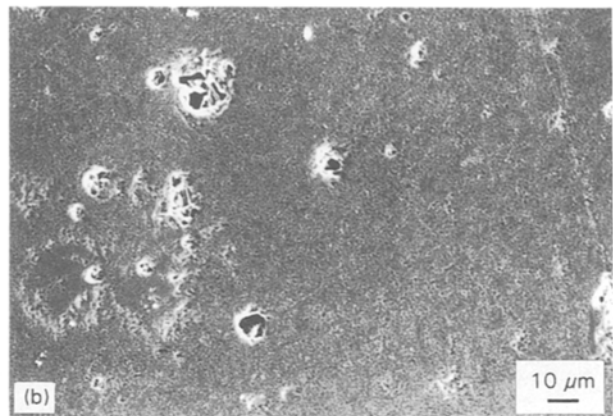
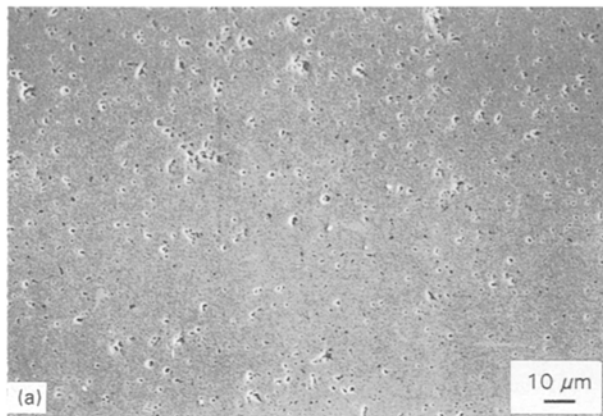


Figure 2 see over page

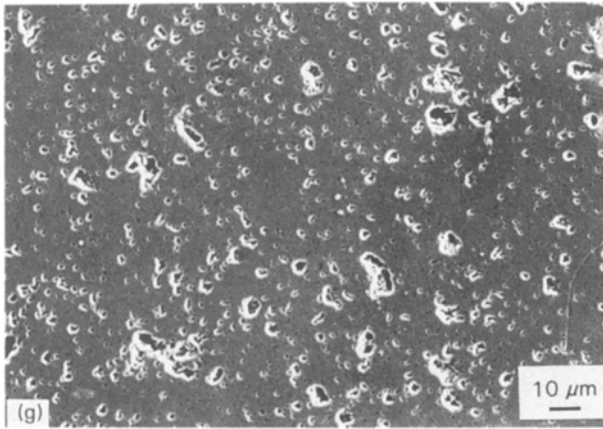
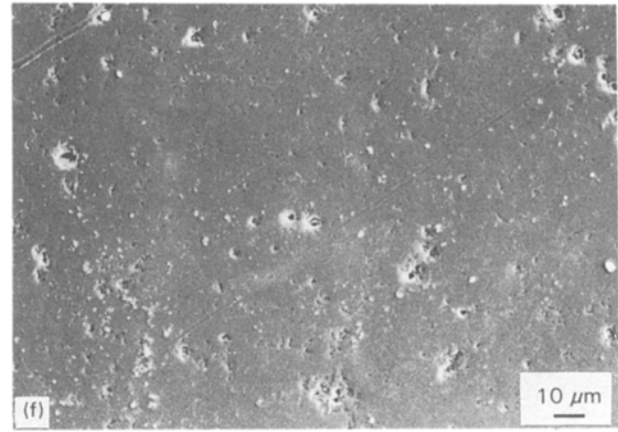
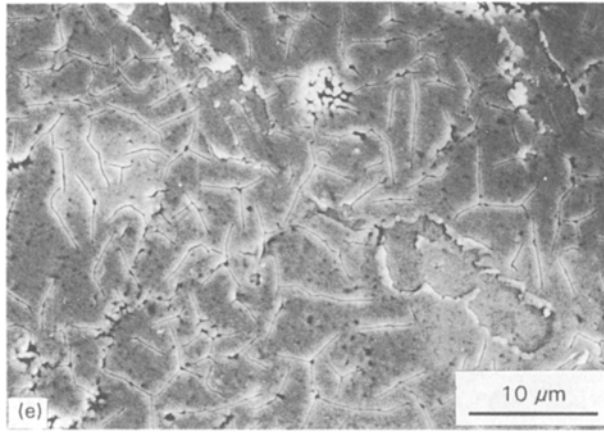


Figure 2 Microstructure of the composition  $\text{Ba}_4(\text{Sm}_{0.6}, \text{Nd}_{0.4})_{9.33}\text{Ti}_{18}\text{O}_{54}$  calcined at  $950^\circ\text{C}$  and sintered at various temperatures in an oxygen flow, with different dopants: (a) undoped,  $1450^\circ\text{C}$ , 2 h; (b) 1 wt %  $\text{WO}_3$ ,  $1450^\circ\text{C}$ , 2 h; (c) 2 wt %  $\text{WO}_3$ ,  $1350^\circ\text{C}$ ; (d) 1 wt %  $\text{MnO}_2$ ,  $1350^\circ\text{C}$ ; (e) 2 wt %  $\text{MnO}_2$ ,  $1350^\circ\text{C}$ . (f) 1 wt %  $\text{CaO}$ ,  $1450^\circ\text{C}$ , 2 h; (g) 2 wt %  $\text{CaO}$ ,  $1450^\circ\text{C}$ , 2 h.

analysis leads to poor microwave properties. The  $\text{CaO}$  prevents the densification. A decrease of  $\epsilon$  and  $Q \times f$  while  $\tau_f$  increases can be observed.

### 3.2. $\text{Ba}_{3.75}(\text{Sm}_{0.5}, \text{Nd}_{0.5})_{9.5}\text{Ti}_{18}\text{O}_{54}$ composition (labelled 2)

#### 3.2.1. Dilatometric study

Dilatometric studies were performed for this composition during sintering with 2 wt % of the three different dopants. The results, shown in Fig. 3, confirm that the reactivity varies with the nature of the dopant.

The reactivity increases in the presence of  $\text{MnO}_2$  and  $\text{WO}_3$ , while the sample doped with  $\text{CaO}$  was found to be difficult to densify well.

These observations led to the use of the following sintering conditions:

(a)  $\text{WO}_3$ -doped sample: sintered at  $1450^\circ\text{C}$  for 2 h in oxygen;

(b)  $\text{MnO}_2$ -doped sample: sintered at  $1350^\circ\text{C}$  for 2 h in oxygen;

(c)  $\text{CaO}$ -doped sample: sintered at  $1450^\circ\text{C}$  for 2 h in oxygen.

#### 3.2.2. Influence of the dopant on the microstructure

Fig. 4 shows the microstructure of ceramics sintered at various temperatures under an oxygen flow. The microstructure of undoped sample shows that the amount of porosity is very small and that a second phase remains. XRD and EDS analysis have been performed in order to identify that secondary phase. The XRD pattern is very difficult to interpret because of the overlapping of the main lines of the different phases. However, the EDS analysis confirms the presence of titanium, samarium and neodymium in the secondary phase in the following amounts:  $\text{Ti} \approx 60\%$ ,  $\text{Sm} \approx 25\%$ ,  $\text{Nd} \approx 15\%$ , which is close to  $(\text{Sm}, \text{Nd})_2\text{-Ti}_2\text{O}_7$ .

TABLE I Microwave characteristics of the  $\text{Ba}_4(\text{Sm}_{0.6}, \text{Nd}_{0.4})_{9.33}\text{Ti}_{18}\text{O}_{54}$  composition versus the nature and amount of dopant

Nature and amount (wt %) of dopant	Sintering temperature ( $^\circ\text{C}$ )	Density $\epsilon$	$Q \times f$ (GHz)	$\tau_f$ (p.p.m. $^\circ\text{C}^{-1}$ )
No dopant	1450	5.40	77 9000	+ 9
1 $\text{WO}_3$	1450	5.64	79.3 8100	+ 10
2 $\text{WO}_3$	1450	5.61	77.4 8100	+ 13
1 $\text{MnO}_2$	1350	5.56	79 6200	+ 10
2 $\text{MnO}_2$	1350	5.63	81.3 4800	+ 14
1 $\text{CaO}$	1450	5.58	79 6500	+ 16
2 $\text{CaO}$	1450	5.12	65 7200	+ 35

3.1.3.2.  $\text{MnO}_2$  effect. The density of the two  $\text{MnO}_2$ -doped samples was higher than the undoped ones, even if these  $\text{MnO}_2$ -doped samples were sintered at lower temperature. This confirms that  $\text{MnO}_2$  acts as a sintering agent for that composition. An increase of  $\epsilon$  can be seen as the dopant amount increases.

The formation of an hypothetical liquid phase at the grain boundary during sintering could explain the good and rapid densification. However, this hypothetical liquid phase is probably ferroelectric or a semiconductor, because the  $Q \times f$  product is low.

3.1.3.3.  $\text{CaO}$  effect. The decrease of the density observed on the microstructure and the dilatometric

3.2.2.1. *WO<sub>3</sub>-doped sample.* The microstructure of this sample shows two secondary phases instead of one for the undoped sample. The third phase is needle-

like, and the length of these needles is about 10 μm. These needles are much too narrow to be analysed by EDS.

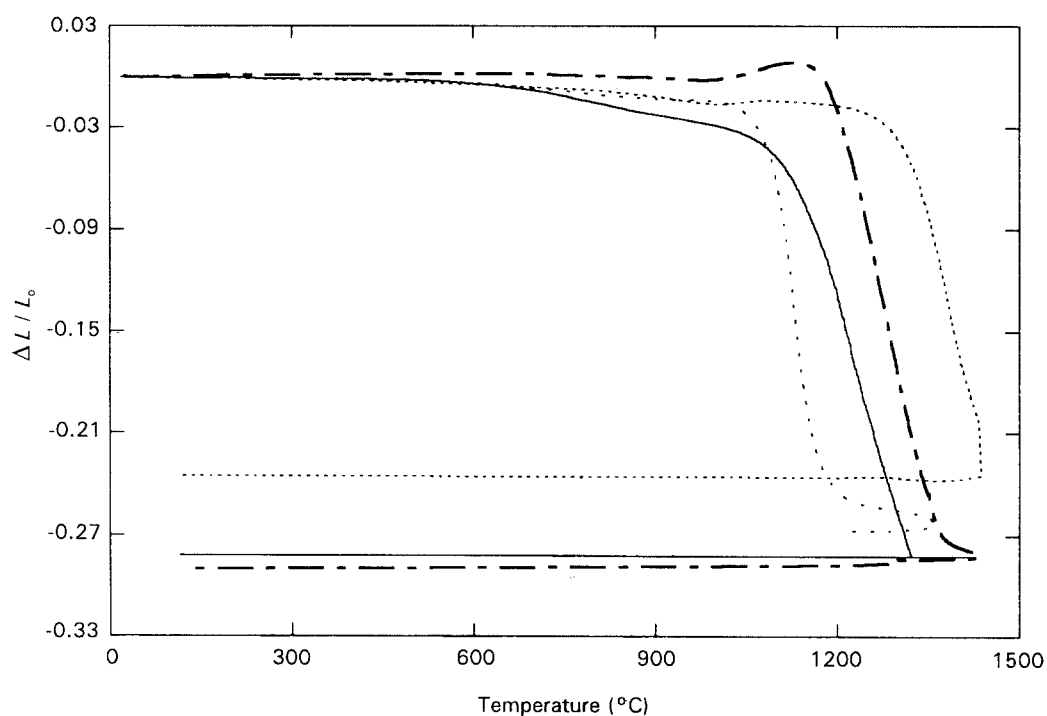


Figure 3 Shrinkage evolution of a pellet of composition Ba<sub>3.75</sub>(Sm<sub>0.5</sub>Nd<sub>0.5</sub>)<sub>9.5</sub>Ti<sub>18</sub>O<sub>54</sub>: calcined at 950°C, sintered in an oxygen flow, with different dopants: (—) 2 wt % WO<sub>3</sub>, (---) 2 wt % MnO<sub>2</sub>, (····) 2 wt % CaO, (-·-·-) no dopant.

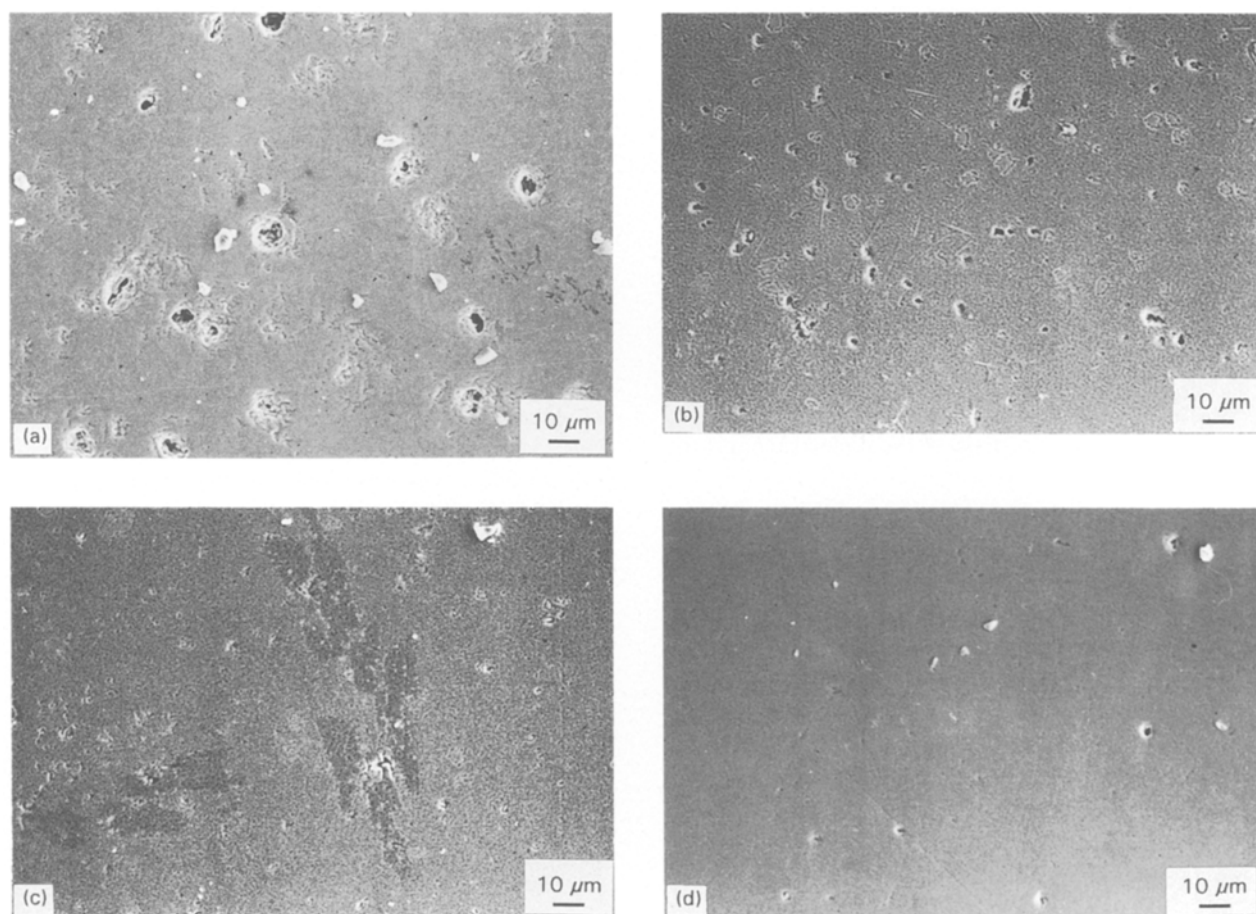


Figure 4 see over page

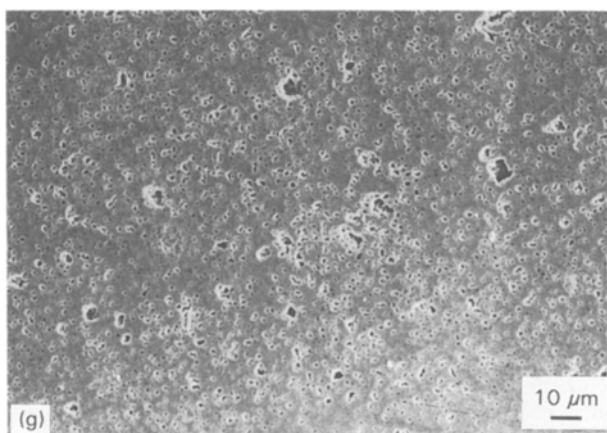
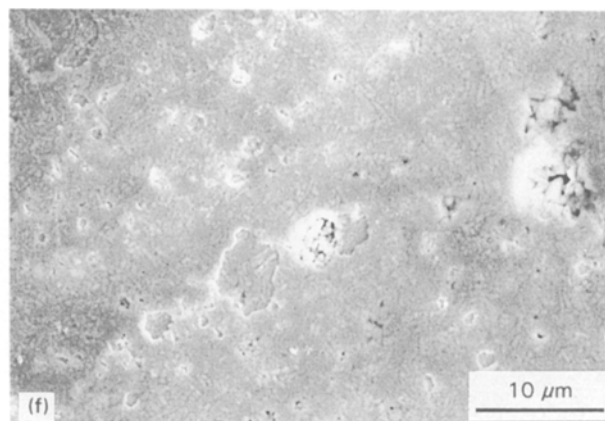
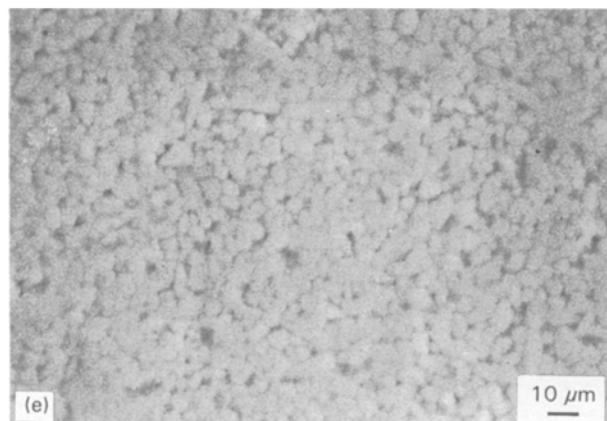


Figure 4 Microstructure of the composition  $Ba_{3.75}(Sm_{0.5}, Nd_{0.5})_{9.33}Ti_{18}O_{54}$  calcined at  $950^{\circ}C$  and sintered at various temperatures in oxygen, with different dopants: (a) Undoped,  $1400^{\circ}C$ , 2 h; (b) 1 wt %  $WO_3$ ,  $1350^{\circ}C$ , 2 h; (c) 2 wt %  $WO_3$ ,  $1350^{\circ}C$ , 2 h; (d) 2 wt %  $MnO_2$ ,  $1350^{\circ}C$ ; (e) 2 wt %  $MnO_2$ ,  $1350^{\circ}C$ ; (f) 1 wt %  $CaO$ ,  $1450^{\circ}C$ , 2 h; (g) 2 wt %  $CaO$ ,  $1450^{\circ}C$ , 2 h.

3.2.2.2. *MnO<sub>2</sub>-doped sample.* This sample shows a pure matrix ceramic for the two amounts of  $MnO_2$ . Some porosity can be seen. The grain size is about  $1 \mu m$ .

3.2.2.3. *CaO-doped sample.* This sample shows a microstructure corresponding to a pure matrix where a large porosity remains. This porosity increases with the amount of dopant.

### 3.2.3. Microwave properties

The microwave characteristics of the doped samples of composition 2 are given in Table II. The sample doped with  $WO_3$  shows a decrease of the dielectric constant,

TABLE II Microwave characteristics of the  $Ba_{3.75}(Sm_{0.5}, Nd_{0.5})_{9.33}Ti_{18}O_{54}$  composition versus the nature and amount of dopant

Nature and amount (wt %) of dopant	Sintering temperature ( $^{\circ}C$ )	Density	$\epsilon$	$Q \times f$ (GHz)	$\tau_f$ (p.p.m. $^{\circ}C^{-1}$ )
No dopant	1400	5.64	81	8700	+ 8.8
1 $WO_3$	1350	5.62	77	7700	19
2 $WO_3$	1350	5.65	75	8100	22
1 $MnO_2$	1350	5.51	80.6	1200	+ 15
2 $MnO_2$	1350	5.62	81	1000	+ 20
1 $CaO$	1450	5.53	79.3	5300	+ 8
2 $CaO$	1450	5.33	74.5	6200	+ 33

$\epsilon$ , and the  $Q \times f$  factor, while the  $\tau_f$  coefficient increases. The evolution of  $\epsilon$  with  $WO_3$  content for this composition (2) is different from that of composition 1. These different evolutions could be attributed to the presence of secondary phases in ceramics of composition 2 instead of pure matrix as observed for composition 1.

The  $MnO_2$  effects are the same as for composition 1: a drastic decrease of  $Q \times f$  and a high coefficient  $\tau_f$ .

Finally, as expected, considering the difficulty of densification during sintering, a degradation of the parameters  $\epsilon$ ,  $Q \times f$  and  $\tau_f$  can be observed when doped with  $CaO$ .

## 4. Conclusion

The effect of adding  $WO_3$ ,  $MnO_2$ ,  $CaO$  to the system  $Ba_{6-x}(Sm_{1-y}Nd_y)_{8+2x/3}Ti_{18}O_{54}$  was studied in terms of microwave properties and microstructural observations. The effects noted in other systems and reported in the literature were rather different in our study. We observed an undeniable effect of the different dopants on reactivity. The effect of  $WO_3$  upon microstructure depends on the composition. In one case, ( $x = 2$ ,  $y = 0.4$ ), no effect was observed. On the other hand, for  $x = 2.25$ ,  $y = 0.5$ , we observed two secondary phases which could not be identified. The microwave properties of those samples show a large dielectric constant, but both  $Q$  and  $\tau_f$  are not improved. The formation of  $BaWO_4$ , which was expected to lower  $\tau_f$ , did not occur. The  $MnO_2$ -doped samples exhibit, whatever the composition, a pure, dense matrix, showing the effect as a sintering agent of this manganese oxide. The density increases, in comparison to the undoped sample, leading to an improvement of the dielectric constant up to 81, a decrease of the quality factor, which is in good agreement with the result of Yamada *et al.* [9]. However, the effect upon the  $\tau_f$  coefficient is different, owing to the absence of the secondary phases, reported by Yamada *et al.* At the least, the

addition of CaO to such compositions leads to a general decrease of the microwaves properties, which is in good agreement with the poor densification of the relative samples.

This study confirms the importance of secondary phases in such a system and, in particular, their influence on the  $Q \times f$  and  $\tau_f$  coefficients.

## References

1. D. KOLAR, *Ber. Deustch Keram. Gess.* **22** (6) (1986), 17.
2. *Idem*, *J. Solid State Chem.* **38** (1981) 158.
3. KAWASHIMA, US Pat. 4330 631 (1982).
4. S. NISHIGAKI, H. KATO, S. YANO, and R. KAMIMURA, *Ceram. Bull.* **66** (1987) 1405.
5. P. LAFFEZ, G. DESGARDIN and B. RAVEAU, *J. Mater. Sci.* **27** (1992) 5229.
6. P. LAFFEZ, G. DESGARDIN, J. M. HAUSSONNE and B. RAVEAU, in *Euroceramic II*, Vol. III, edited by G. Ziegler and H. Hausner (Köln Publishers, Germany, 1991) pp. 2043–47.
7. S. NISHIGAKI, S. YANO, H. KATO, T. HIRAI and T. NONOMURA, *J. Am. Ceram. Soc.* **71** (1988) C11-C17.
8. K. WAKINO, K. MINAI and H. TAMURA, *ibid.* **67** (1984) 278.
9. A. YAMADA, Y. UTSUMI and H. WATARAI, *Jpn J. Appl. Phys.* **30** (1991) 2350.
10. G. S. MHAISALKAR, D. W. READEY and S. A. AKBAR, *J. Am. Ceram. Soc.* **74** (1991) 1894.
11. T. NEGAS, G. YEAGER, S. BELL and R. AMREN, "Chemistry and Properties of compensated microwave dielectrics", National Institute of Standards and Technology, special publication 804 National Institute of Standards and Technology, Jackson, WY, (1990) p. 17.
12. B. W. HAKKI and P. D. COLEMAN, *IRE Trans. Microwave Theory Techn.* July (1959) 402.

*Received 13 July 1993  
and accepted 16 May 1994*